Journal of Luminescence 36 (1986) 101–107
North-Holland, Amsterdam

THE IMPACT CROSS SECTION OF Er^{3+} IN ZnS

Xu-mou XU, Jia-qi YU and Guo-zhu ZHONG

Changchun Institute of Physics, Academia Sinica, People's Rep. China

Received 8 October 1985
Revised 14 July 1986
Accepted 21 July 1986

Four kinds of Er^{3+} centers in $ZnS:Er^{3+}$ thin films have been distinguished by means of laser selective excitation. Their impact cross sections in electroluminescence (EL) and absorption cross sections in photoluminescence (PL) have been compared with each other. The average value of the impact cross section of Er^{3+} obtained by comparing the EL intensity of Er^{3+} with that of Mn^{2+} in $ZnS:ErF_3$, Mn^{2+} thin films is about 2×10^{-16} cm^2.

1. Introduction

The impact cross section of luminescent centers is a very important parameter for EL in which impact excitation by hot electrons is the dominant mechanism. Some authors have studied this problem theoretically, put forward a few methods to calculate the cross section approximately, and calculated the cross section of Mn^{2+} [1–4]. But only Muller and Mach [5] directly obtained the cross section of Mn^{2+} in ZnS thin films experimentally. No direct experimental result about the impact cross section of rare earth ions in EL devices has been gained up to now.

In this paper research on the impact cross section of Er^{3+} in ZnS is reported. We have used high-resolution spectroscopy under laser selective excitation and electric field excitation to study $ZnS:Er^{3+}$ thin films, distinguished four luminescent centers, and compared their cross sections. By comparing the EL intensities of Er^{3+} and Mn^{2+} in $ZnS:ErF_3$, Mn^{2+} thin films, we have obtained the relative ratio of the impact cross section of Er^{3+} to that of Mn^{2+}, and further calculated the impact cross section of Er^{3+} which, to our belief, is the first experimental result for the impact cross section of Er^{3+} in ZnS.

2. Samples and experimental set up

The structures of samples used in the experiments are ITO–Y_2O_3–$ZnS:Er^{3+}$–Al and ITO–Y_2O_3–$ZnS:ErF_3$, Mn^{2+}–Y_2O_3–Al ("ITO" is a transparent conductive layer with In_2O_3 95% and SnO_2 5%). Glass is used as substrate. Before evaporation, the materials had been fired for about two hours at around 1000°C. The Y_2O_3 was fired in air after being pressed into slices, and the ZnS in S atmosphere. When the Mn^{2+} doped samples were fabricated, the $MnCl_2$ was mixed into the ZnS powder, the mixture was ground mechanically and then fired in S atmosphere.

The Y_2O_3 layer with a thickness of about 300 nm was fabricated by electron-beam evaporation. The 0.5–1 μm luminescent layer was made by co-evaporation of ZnS and dopants from separate boats. During evaporation, the substrate temperature was 160–200°C, and the vacuum was around 2×10^{-5} Torr.

A NRG–PTL–2000 dye laser pumped by a N_2 laser was used as excitation light source in the PL experiment. Coumarin 485 was used. The line width of the laser is about 1.2 cm^{-1}. The luminescence after passing a Spex 1403 double-grating spectrometer was received by a thermoelectrically

0022-2313/86/$03.50

cooled C31034 photomultiplier, and fed into the Datamate photon counting system. When time resolved spectra were measured, a PAR 162/165 Boxcar was used.

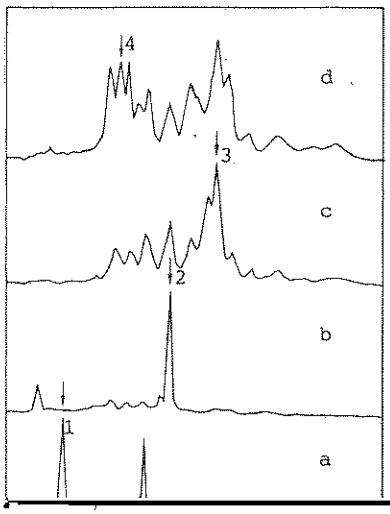

3. Results and discussion

3.1. Comparison between the impact cross section of different Er^{3+} centers

(1) *Different Er^{3+} centers*

The AC EL spectra ($^4S_{3/2} - {}^4I_{15/2}$ transition) of many ZnS : Er^{3+} samples have been measured at liquid nitrogen temperature. Figure 1 shows a typical spectrum. The spectra are complex with

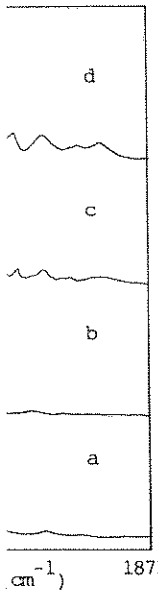

ectra at 77 K. (1) 19124 cm^{-1}, (4) 19055 cm^{-1}.

111 and 18119 cm^{-1} pectra have also been kinds of spectra, four

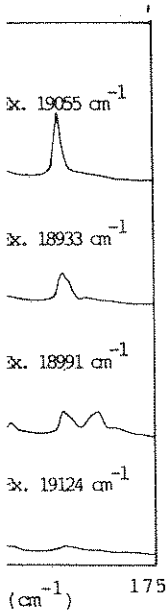

lines excitation at 77 K. (1) 1) 18111 cm^{-1}, (4) 18119

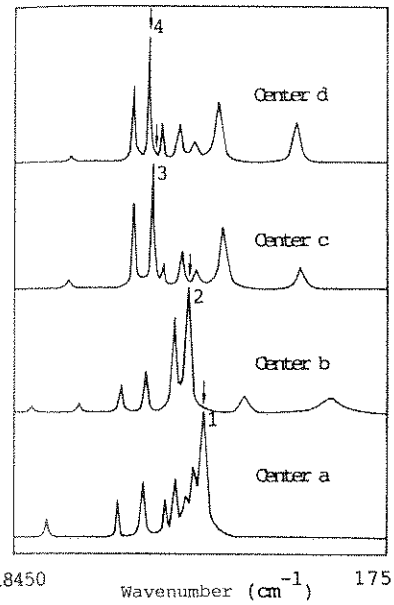

Fig. 4. Decomposed spectra of four centers. (1) 17991 cm^{-1}, (2) 18027 cm^{-1}, (3) 18111 cm^{-1}, (4) 18119 cm^{-1}.

major luminescent centers were identified. Based on the main emission lines of these four centers, the emission spectra were decomposed into the spectra of centers a, b, c and d by iteration and best fitting methods. The decomposed spectra are shown in fig. 4. The spectra of centers c and d are very similar, but they are indeed two different centers. The identification is supported by the fact that the 18111 cm^{-1} line of center c decays slower than 18119 cm^{-1} line of center d, and the positions of lines of center c and the relevant ones of center d, though very near to each other, are about 10 cm^{-1} different. They may come from similar centers.

(2) *Determination of the relative concentrations of the different centers*

The $^2H_{11/2}$ and $^4S_{3/2}$ are two primary transition levels of Er^{3+}. Since direct excitation of $^4S_{3/2}$ is more difficult, in the experiment the excited level is $^2H_{11/2}$ and the monitored emission level is $^4S_{3/2}$. In this case, a three-level model of Er^{3+} can be set up as shown in fig. 5. Here N is the total number of luminescent centers; n_1, n_2 are the numbers of centers being in $^2H_{11/2}$ and $^4S_{3/2}$,

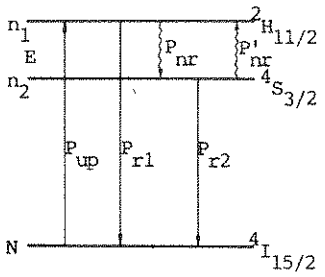

Fig. 5. Three-level model of Er^{3+}.

respectively; P_{r1}, P_{r2} the radiative transition probabilities from $^2H_{11/2}$ and $^4S_{3/2}$ to the ground state $^4I_{15/2}$; P_{nr}, P'_{nr} the down- and up-transition probabilities between two excited states, respectively; P_{up} is the excitation probability from the ground state to $^2H_{11/2}$; E is the energy difference between $^2H_{11/2}$ and $^4S_{3/2}$.

$^2H_{11/2}$ is very near to $^4S_{3/2}$, so it can be assumed that they are in thermal equilibrium. According to the model, under pulse laser excitation, the integrated intensities I_1 of $^2H_{11/2}$–$^4I_{15/2}$ and I_2 of $^4S_{3/2}$–$^4I_{15/2}$ transition are

$$I_1 = \frac{\alpha N P_{up} P_{r1}\,\Delta t}{T(\alpha W_1 + W_2)}, \tag{1}$$

$$I_2 = \frac{N P_{up} P_{r2}\,\Delta t}{T(\alpha W_1 + W_2)}. \tag{2}$$

$\alpha = (g_1/g_2)\exp(-E/KT)$ ($g = 2J_1 + 1 = 12$, $g_2 = 2J_2 + 1 = 4$ are the degeneracies of the two levels, respectively), W_1 and W_2 are the transition probabilities from $^2H_{11/2}$ and $^4S_{3/2}$ to all levels below $^4S_{3/2}$ respectively, T and Δt the period and width of the laser pulse, respectively.

Dividing (1) by (2) yields

$$I_1/I_2 = \alpha P_{r1}/P_{r2}. \tag{3}$$

Because the concentration of Er^{3+} in the samples is low, the interactions between different centres can be neglected; energy transfer from luminescent centers to quenching centers is also neglected. The distance between $^4S_{3/2}$ and the nearest level $^4F_{9/2}$ is about 3000 cm^{-1}, much larger than the phonon energy of ZnS, so that, the multiphonon relaxation to the levels below $^4S_{3/2}$ can also be ignored. Thus, W_1 and W_2 are radiative transition probabilities.

The relationship between P_{r2} and W_2 is

$$P_{r2} = \beta_2 W_2.$$

β is the fluorescent branching ratio which can be calculated using the published Ω parameters and reduced matrix elements. Since the difference between the wave functions of rare earth ions in different hosts is not large, the reduced matrix elements given by ref. [6] have been used. The Ω parameters are from ref. [7]. The calculated result is $\beta_2 = 0.700$.

Measuring the decay time τ_2 of $^4S_{3/2}-{}^4I_{15/2}$ emission at 77 K, the radiative transition probability $W_2 = 1/\tau_2$ can be obtained. P_{r2} can be obtained from $\beta_2 W_2$.

According to formula (3), from the relative intensities of I_1 and I_2 at different temperatures, the magnitude of P_{r1}^{-1} can be obtained by the least-square method.

Table 1 gives the measured and calculated data of the four samples. At liquid nitrogen temperature, $\alpha = 4 \times 10^{-5}$, and $I_1 \ll I_2$, $\alpha W_1 \ll W_2$, thus, formula (2) can be written, approximately, as

$$I_2 = \frac{1}{TW_2} NP_{up} P_{r2}\, \Delta t = \frac{1}{T} NP_{up}\beta_2\, \Delta t. \tag{4}$$

On the basis of the Einstein formula $P_{up} = (c^3/8\pi h\nu^3)P_r J(\nu)$ (where $J(\nu) = 2\pi\rho(\nu)$ is the excitation density, $\rho(\nu) = Fn/c$, n is the refractive index of the medium, F the intensity of the excitation light), formula (4) may be written as

$$I_2 \propto KNF\beta_2\, \Delta t/\left(T\nu^3 P_{r1}^{-1}\right), \tag{5}$$

where $K = \Delta\nu/\Delta\nu_L$, $\Delta\nu$ is the line width of the excitation spectrum, $\Delta\nu_L$ is the laser line width.

The ratio of the concentrations of centers a and b is as follows:

$$\frac{N_a}{N_b} = \frac{I_a \nu_a^3 P_{ra}^{-1} F_b}{I_b \nu_b^3 P_{rb}^{-1} F_a}, \tag{6}$$

where we assume that K is equal for center a and center b as an approximation.

The absorption cross section of a luminescent center $S \propto P_{up}/F$, then the ratio of absorption cross sections can be obtained

$$\frac{S_a}{S_b} = \frac{P_{up(a)} F_b}{P_{up(b)} F_a} = \frac{P_{rb}^{-1}\nu_b^3}{P_{ra}^{-1}\nu_a^3}. \tag{7}$$

Decomposing the spectra shown in fig. 3, the relative intensities of the four centers in the samples have been obtained. Meanwhile, measuring the intensities of the four laser lines, using formulae (6) and (7) and the data listed in table 1 the relative concentrations and absorption cross sections of the four centers have been gained. The results are listed in table 2.

(3) *Comparison between the impact cross sections of different centers*

Direct impact excitation is the excitation mechanism of the samples under electric field excitation, the number of centers excited to an upper state within unit time is $CN\int n_0 f(E) v(E) \sigma(E)\, dE$, where n_0, $f(E)$, $v(E)$ are the density, distribution function and velocity of hot electrons, respectively; $\sigma(E)$ is the impact cross section of luminescent centers, C is a constant related to the sample's structure and field's distribution. The dynamical equation is

$$\frac{dn}{dt} = CN\int n_0 f(E) v(E) \sigma(E)\, dE - nP_r.$$

Under steady excitation, $dn/dt = 0$, then $CN\int n_0 f(E) v(E) \sigma(E)\, dE - nP_r = 0$. However, $I = nP_r$, therefore

$$I \propto N\int n_0 f(E) v(E) \sigma(E)\, dE.$$

The impact cross section is a complicated parameter. The cross section considered here is the average value corresponding to the two major

Table 1
Values of τ_2 and P_{r1}^{-1} of four centers

Sample	Center	a	b	c	d
1	τ_2 (μs)	49	139	228	174
	P_{r1}^{-1} (μs)	6.2	17	25	18
2	τ_2 (μs)	49	138	225	171
	P_{r1}^{-1} (μs)	5.2	12	20	14
3	τ_2 (μs)	50	128	208	158
	P_{r1}^{-1} (μs)	5.9	12	20	14
4	τ_2 (μs)	51	147	244	187
	P_{r1}^{-1} (μs)	5.7	15	24	19
Average value	τ_2 (μs) (±10%)	50	138	226	173
	P_{r1}^{-1} (μs) (±20%)	5.7	14	22	16

Table 2
Intensities of PL and

Sample	C
	L
	F
	(ν
1	Pl
2	(r.
3	
4	
1	El
2	(r.
3	
4	
1	C
2	(r.
3	
4	
1	O
2	S
3	
4	
Average S (r.u.) (±3	
1	In
2	σ
3	
4	
Average σ (r.u.) (±4	

transition levels
formula above m

$$I \propto N\sigma \int n_0 f(E)$$

Since the frec
$^4S_{3/2}-{}^4I_{15/2}$ for
the integrands in
can be considered

$$\frac{\sigma_a}{\sigma_b} = \frac{I_a N_b}{I_b N_a}.$$

Decomposing
emission spectra
4), the relative E
are obtained. Usi
cross sections of
listed in table 2.
caused mainly by
position of the sp

Table 2
Intensities of PL and EL, concentrations, absorption and impact cross sections of four centers in samples 1–4

Sample	Center	a	b	c	d
	Laser line (cm^{-1})	19124	18991	18933	19055
	F (r.u.)	1.02	1.04	1	1.06
	(ν_i/ν_c)	1.03	1.01	1	1.02
1	PL intensity	7.5	7.4	10	5.7
2	(r.u.)	7.4	9.0	10	7.3
3		5.0	12.3	10	8.3
4		3.3	6.3	10	5.4
1	EL intensity	7.6	12.8	10	9.8
2	(r.u.)	6.3	13.4	10	13.8
3		5.5	14.6	10	13.1
4		2.9	8.3	10	9.8
1	Concentration	2.0	4.6	10	4.0
2	(r.u.)	1.9	5.6	10	5.1
3		1.3	7.6	10	5.8
4		0.9	3.9	10	3.8
1	Optical absorption cross section	4.0	1.5	1	1.4
2	S (r.u.)	3.7	1.7	1	1.4
3		3.3	1.7	1	1.4
4		4.1	1.6	1	1.2
Average S (r.u.) (±30%)		3.8	1.6	1	1.4
1	Impact cross section	3.8	2.8	1	2.5
2	σ (r.u.)	3.3	2.4	1	2.7
3		4.2	1.9	1	2.3
4		3.2	2.1	1	2.6
Average σ (r.u.) (±45%)		3.6	2.3	1	2.5

transition levels $^2H_{11/2}$ and $^4S_{3/2}$ of Er^{3+}, so the formula above may be rewritten as

$$I \propto N\sigma \int n_0 f(E) v(E)\, dE. \tag{9}$$

Since the frequency differences of transition $^4S_{3/2}$–$^4I_{15/2}$ for different centers are very small, the integrands in formula (9) for different centers can be considered equal. Then we have

$$\frac{\sigma_a}{\sigma_b} = \frac{I_a N_b}{I_b N_a}. \tag{10}$$

Decomposing the EL spectra (fig. 1) into the emission spectra of four centers a, b, c and d (fig. 4), the relative EL intensities of the four centers are obtained. Using formula (10), relative impact cross sections of them are gained. The results are listed in table 2. The uncertainty of S and σ are caused mainly by the uncertainty in the decomposition of the spectra.

It can be seen from these data that the impact and absorption cross sections are both about 4 times different and their variations with centers are similar, though not the same. As we know, the magnitude of absorption cross section is mainly dependent on the transition probability. The experimental results indicate that the impact cross sections of different centers formed with the same dopant are primarily dependent on their transition probabilities, their structures might have a secondary effect.

3.2. The impact cross section of Er^{3+}

In the previous section, only the relative magnitudes of cross sections for different centers of Er^{3+} have been studied. The following experiments are designed to determine the absolute value of the impact cross section of Er^{3+}. The principle of the experiments is that the relative ratio of the

cross sections of Er^{3+} and Mn^{2+} is obtained first by comparing their EL intensities in $ZnS:ErF_3$, Mn^{2+} thin films, then the cross section of Er^{3+} is calculated using the cross section of Mn^{2+} obtained by Muller [5].

In order to avoid significant energy transfer between Er^{3+} and Mn^{2+}, the concentrations of Er^{3+} and Mn^{2+} in the samples are low, within the range of 5×10^{-5}–5×10^{-4} mol/mol ZnS.

We have already determined that erbium centers formed by ErF_3 doping in our samples are not ErF_3 molecular centers but complex centers consisting of Er^{3+} and F^{1-}, which have similar impact cross section as erbium centers formed by metal Er doping [8].

It has been proved that direct impact excitation by hot electrons is the major mechanism in TF devices doped with rate earth ions [9]. Under this condition, in formula (9), for the intensity of emission lines from a certain manifold, the integral should be over the energy range of hot electrons which can excite the luminescent centers to this manifold.

For Mn^{2+} we take the zero phonon line 17 891 cm^{-1} in the emission spectrum to be the lower integral limit, for Er^{3+} we take the strongest emission line 18 135 cm^{-1} of the $^4S_{3/2}$–$^4I_{15/2}$ transition as the lower integral limit. The upper integral limit should be the nearest high level having strong emission. Above the zero phonon line, Mn^{2+} has no emission, but five continuous excitation bands. Above the $^2H_{11/2}$ level, Er^{3+} has many excited states, but there is no strong emission from these levels in EL in our experiment. It implies that electrons excited to higher levels will relax to $^2H_{11/2}$ and $^4S_{3/2}$. We take ∞ as the upper integral limit. Thus, the two upper integral limits are the same, while the energy difference of the two lower limits $E \doteq 250$ $cm^{-1} = 0.03$ eV, is quite small compared with the average energy of hot electrons, 0.15 eV [7], so that the two integrations may be regarded equal to each other. Based on formula (9), the relative ratio of impact cross sections of the two ions is approximately

$$\sigma_{Er}/\sigma_{Mn} = I_{Er}N_{Mn}/I_{Mn}N_{Er}. \qquad (11)$$

At 77 K, EL spectra of four $ZnS:ErF_3$, Mn^{2+} samples and a $ZnS:Mn^{2+}$ sample have been measured as shown in fig. 6. Decomposing the spectra, relative values of I_{Er} and I_{Mn} have been obtained. I_{Er} is the integrated area of the Er^{3+} emission spectra. Different Er^{3+} centers are not distinguished. The concentrations of Er^{3+} and Mn^{2+} in these samples were determined by the induction coupled plasma atomic emission spectroscopy. Using formula (11), the relative ratio of the impact cross sections of Er^{3+} and Mn^{2+} is calculated.

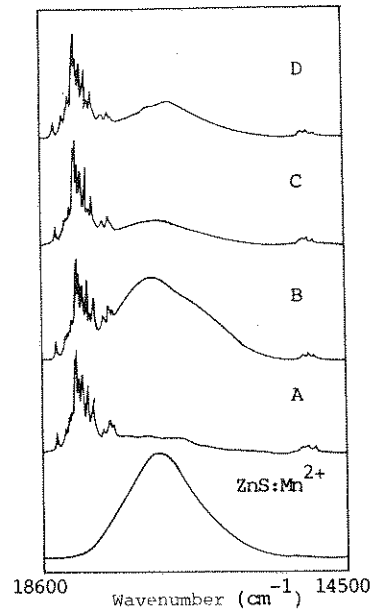

Fig. 6. AC EL spectra of four $ZnS:ErF_3$, Mn^{2+} TFs and a $ZnS:Mn^{2+}$ TF at 77 K.

Using the impact cross section of Mn^{2+} in ZnS

Table 3
Values of parameters of $ZnS:ErF_3$, Mn^{2+} TFs

Samble	A	B	C	D
N_{Er} ($\times10^{-4}$ mol) ($\pm$20%)	5.2	0.6	1.5	1.7
N_{Mn} ($\times10^{-4}$ mol) ($\pm$20%)	3.5	1.8	1.0	1.8
Excitation voltage (V)	227	231	247	217
I_{Er} (r.u.)	1.0	1.0	1.0	1.0
I_{Mn} (r.u.)	1.2	6.5	1.4	2.3
σ_{Er}/σ_{Mn}	0.56	0.46	0.48	0.46
σ_{Er} ($\times10^{-16}$ cm^2) ($\pm$30%)	2.2	1.8	1.9	1.8

Table 4
Relationship between

Voltage	193
I_{Er} (r.u.)	1.0
I_{Mn} (r.u.)	2.3
σ_{Er}/σ_{Mn}	0.46

$\sigma_{Mn} = 4.0\times10^{-16}$
the impact cross s
data is given in tal
Taking the aver
$\sigma_{Er} = 2\times10^{-16}$ cm
The impact cr
that of Mn^{2+}. C
range of the wav
radius of Er^{3+} a
Mn^{2+}, σ_{Mn} shoul
considering that
electrons excited t
also be affected b
bigger the σ may
constant of emissi
cm^{-1} at 77 K,
$^4S_{3/2}$–$^4I_{15/2}$ emissi
proximation, takin
their time constant
probabil-
ities, the P_{up} of E
than that of Mn^{2+}
radius of 3d and 4
that σ_{Er} for $^4S_{3/2}$ i
The relative rat
of Er^{3+} and Mn^{2}
termined from th

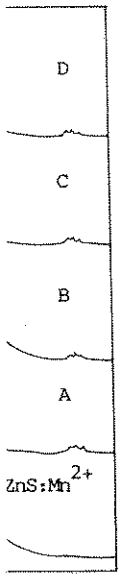

(cm^{-1}) 14500

S:ErF_3, Mn^{2+} TFs and a
at 77 K.

6. Decomposing the
ir and I_{Mn} have been
ted area of the Er^{3+}
Er^{3+} centers are not
rations of Er^{3+} and
re determined by the
itomic emission spec-
), the relative ratio of
of Er^{3+} and Mn^{2+} is

ction of Mn^{2+} in ZnS,

, Mn^{2+} TFs

B	C	D
0.6	1.5	1.7
1.8	1.0	1.8
231	247	217
1.0	1.0	1.0
6.5	1.4	2.3
0.46	0.48	0.46
1.8	1.9	1.8

Table 4
Relationship between impact cross section and voltage

Voltage	193	199	204	217	221	225
I_{Er} (r.u.)	1.0	1.0	1.0	1.0	1.0	1.0
I_{Mn} (r.u.)	2.3	2.4	2.4	2.3	2.3	2.3
σ_{Er}/σ_{Mn}	0.46	0.44	0.44	0.46	0.46	0.46

$\sigma_{Mn} = 4.0 \times 10^{-16}$ cm^2, measured by Muller [5], the impact cross section of Er^{3+} is obtained. The data is given in table 3.

Taking the average value for the samples, yields

$\sigma_{Er} = 2 \times 10^{-16}$ cm^2 ($\pm 30\%$).

The impact cross section of Er^{3+} is close to that of Mn^{2+}. Only considering the spreading range of the wave function, i.e. the 4f electron radius of Er^{3+} and the 3d electron radius of Mn^{2+}, σ_{Mn} should be much larger than σ_{Er}. But considering that σ is defined by the number of electrons excited to upper level in unit time, should also be affected by P_{up} and the larger the P_{up}, the bigger the σ may be. We have measured the time constant of emission of Mn^{2+} excited by 19197 cm^{-1} at 77 K, $\tau_{Mn} = 1.55$ ms, and that of $^4S_{3/2}$–$^4I_{15/2}$ emission of Er^{3+}, 269 μs. As an approximation, taking the ratio of the reciprocals of their time constants as the ratio of their excitation probabilities, the P_{up} of Er^{3+} is about one order larger than that of Mn^{2+}, which offsets the effect of the radius of 3d and 4f electrons, making it possible that σ_{Er} for $^4S_{3/2}$ is close to σ_{Mn}.

The relative ratios of the impact cross section of Er^{3+} and Mn^{2+} in sample D have been determined from threshold voltage to saturation voltage. The results are listed in table 4. It can be seen that the ratio does not vary with voltage.

4. Conclusion

(1) There exist differences between the impact cross sections of different centers formed with the same rare earth dopant, which are primarily caused by differences of their transition probabilities.

(2) The average value of the impact cross section of Er^{3+} in ZnS is about 2×10^{-16} cm^2, close to that of Mn^{2+}, which is due to its larger excitation probability.

Acknowledgement

The authors wish to thank Mr. Huang Shi-hua for his assistance in the experiments and fruitful discussions, Mr. Zhao Guo-zhang for his help with the preparation of the sample.

References

[1] F. Williams et al., Proc. SID, 24/2 (1983) 108.
[2] J.W. Allen, J. Lumin. 23 (1981) 127.
[3] J.E. Bernard, M.F. Martens and F. Williams, J. Lumin. 24/25 (1981) 893.
[4] W.E. Hagston, Phys. Status Solidi (a) 81 (1984) 687.
[5] R. Mach and G.O. Muller, Phys. Status Solidi (a) 81 (1984) 609.
[6] W.T. Carnall et al., Energy Level Structure and Transition Probabilities in the Spectra of Trivalent Lanthanides in LaF_3 (Argonne National Laboratory, 1978).
[7] G.Z. Zhong and F.J. Bryant, J. Lumin. 24/25 (1981) 909.
[8] Xu Xu-mou, Thesis, Changchun Institute of Physics, 1985.
[9] G.O. Muller, Phys. Status Solidi (a) 81 (1984) 597.